

Received May 21, 2019, accepted June 19, 2019, date of publication June 24, 2019, date of current version July 15, 2019.

Digital Object Identifier 10.1109/ACCESS.2019.2924720

# Optimum Deployment of Multiple UAVs for Coverage Area Maximization in the Presence of Co-Channel Interference

AZIZ A. KHUWAJA<sup>1,2</sup>, GAN ZHENG<sup>3</sup>, (Senior Member, IEEE),  
YUNFEI CHEN<sup>1</sup>, (Senior Member, IEEE),  
AND WEI FENG<sup>4,5</sup>, (Senior Member, IEEE)

<sup>1</sup>School of Engineering, The University of Warwick, Coventry CV4 7AL, U.K.

<sup>2</sup>Department of Electrical Engineering, Sukkur IBA University, Sukkur 65200, Pakistan

<sup>3</sup>Wolfson School of Mechanical, Electrical, and Manufacturing Engineering, Loughborough University, Loughborough LE11 3TU, U.K.

<sup>4</sup>Peng Cheng Laboratory, Shenzhen 518000, China

<sup>5</sup>Beijing National Research Center for Information Science and Technology, Tsinghua University, Beijing 100084, China

Corresponding author: Wei Feng (fengwei@tsinghua.edu.cn)

This work was supported in part by the Beijing Natural science Foundation under Grant L172041, in part by the National Science Foundation of China under Grant 61771286, Grant 61701457, Grant 91638205, and Grant 61671478, and in part by the Beijing Innovation Center for Future Chip. The work of G. Zheng was supported in part by the U.K. EPSRC under Grant EP/N007840/1, and in part by the Leverhulme Trust Research Project under Grant RPG-2017-129.

**ABSTRACT** The use of the unmanned aerial vehicle (UAV) as the aerial base stations can provide wireless communication services in the form of UAV-based small cells (USCs). Thus, the major design challenge that needs to be addressed is the coverage maximization of such USCs in the presence of co-channel interference generated by multiple UAVs operating within a specific target area. Consequently, the efficient deployment strategy is imperative for USCs while optimizing the coverage area performance to compensate for the impact of interference. To this end, this paper presents a coordinated multi-UAV strategy in two scenarios. In the first scenario, symmetric placement of UAVs is assumed at a common optimal altitude and transmit power. In the second scenario, asymmetric deployment of UAVs with different altitudes and transmit powers is assumed. Then, the coverage area performance is investigated as a function of the separation distance between UAVs that are deployed in a certain geographical area to satisfy a target signal-to-interference-plus-noise ratio (SINR) at the cell boundary. Finally, the system-level performance of a boundary user is studied in terms of the coverage probability. The numerical results unveil that the SINR threshold, the separation distance, and the number of UAVs and their formations should be carefully selected to achieve the maximum coverage area inside and to reduce the unnecessary expansion outside the target area. Thus, this paper provides important design guidelines for the deployment of multiple UAVs in the presence of co-channel interference.

**INDEX TERMS** Coverage area performance, interference management, UAV-based small cells, UAV communications, UAV separation distance.

## I. INTRODUCTION

Unmanned aerial vehicles (UAVs) equipped with radio transceivers can satisfy the requirements for an aerial communication platform by serving either as a mobile base station or as an airborne relay. Due to their flexible deployment, UAVs can be used in multi-tier UAV-assisted cellular networks to provide on-demand communication services in disaster areas and to enhance coverage, capacity

The associate editor coordinating the review of this manuscript and approving it for publication was Yupeng Wang.

and reliability performances of existing terrestrial cellular networks [1]. However, several challenges, such as optimal 3D placement, flight endurance time, energy constraints and interference management, may impede the widespread applicability of UAV communications [2].

In UAV communications, an aerial base station is mostly a low altitude platform to provide ground coverage as UAV-based small cells (USCs). The size of USCs varies according to the altitude, position, transmit power, and type of UAVs and characteristics of the environment. In this regard, the optimum placement of UAVs to analyze the

coverage performance of USCs has attracted great research interest. For instance, in [3] and [4], the UAV deployment issue has been considered for the coverage enhancement of a single USC. In [5], the authors presented the UAV placement method in a 3D space to enlarge the coverage area. References [6] and [7] analyzed the optimal UAV altitude to maximize the coverage area with minimum outage probability for a given signal-to-noise ratio (SNR) threshold. In [8], the authors analyzed the optimization problem for UAV placement to increase the number of covered users with various quality-of-service (QoS) demands. However, these works were conducted for networks with a single UAV. When multiple UAVs are available, references [9] and [10] exploited the deployment of multiple UAVs to reduce the number of aerial base stations and expand coverage for the ground users. Furthermore, most of the works either optimize the horizontal coordinates of UAVs for a constant UAV altitude above the ground [11] or optimize the UAV altitude while keeping a constant horizontal position [12], [13]. These studies analyzed the UAV placement problem using optimization framework in an interference-free environment. However, in the multi-UAV scenario, interference may be inevitable, as spectrum scarcity may necessitate frequency reuse over the spatial domain [14], causing interference in UAV-assisted cellular networks. Therefore, effective interference mitigation framework is required to maximize the coverage performance and guarantee reliable communications.

#### A. RELATED WORK AND MOTIVATION

From the perspective of UAV communications, several works have been carried out to characterize the interference generated by UAVs and the impact of interference from terrestrial base stations on the UAV connectivity. For example, the authors in [15] presented the interference-aware placement strategy for UAV relays to overcome traffic congestion and to compensate outage in LTE networks. In [16], the authors analyzed the coverage performance of USCs with and without interference for two UAVs. References [17] and [18] used the empirical measurements to characterize the impact of UAV altitude on interference incurred by the terrestrial Long Term Evolution (LTE) networks. In [19], simulation was carried out using commercial software to study the effect of UAV altitude on coverage area and inter-cell interference. Reference [20] proposed the deployment method for multiple UAVs using circle packing theory to maximize the coverage performance and to compensate interference with the adjustment in UAV's altitude and the gain of directional antenna. In [21], the interference alignment principle was exploited to manage the interference in small-cell networks. In [22], circle placement problem was formulated without considering coverage overlapping to avoid interference and to achieve maximum user coverage and power efficiency. Most of these studies have relaxed the overlapping coverage constraints to avoid the co-channel interference. Also, the separation distance between UAVs is an important parameter that determines the trade-off between coverage and interference

generated by UAVs but no comprehensive results are available in the literature to study this parameter in the multi-UAV network.

In UAV communication, the co-channel interference primarily occurs when multiple UAVs share the same frequency resources at the same time in spatially separated locations. Therefore, some research efforts have been devoted to consider the effect of co-channel interference in the performance analysis of UAV communication. For example, reference [23] considered the impact of the co-channel interference in the problem formulation of the UAV trajectory optimization. Reference [24] took into account the effect of co-channel interference between different data user streams in ground-to-UAV uplink transmission. In [25], the authors derived the closed-form expression of the ground user coverage probability to characterize the influence of co-channel interference while capturing the effect of density of UAV deployment, UAV antenna beam-width and the optimum altitude. On the other hand, interference management techniques have been proposed in the existing literature. For example, in [26], the multi-antenna UAV scheme was proposed as the co-channel interference cancellation technique. Furthermore, references [27] and [28] demonstrated that caching can be used for interference management in UAV communication. In reference [29], the coordinate multipoint (CoMP) architecture was exploited for multi-UAV system to mitigate interference and offer high UAV mobility. In [30], the path-planning algorithm was proposed to achieve a trade-off between the maximization of energy efficiency and minimization of both the interference and latency. In [31], the cooperative non-orthogonal multiple access (NOMA) was proposed to mitigate the uplink interference in cellular-connected UAV communication. However, these techniques may require excessive power for signal processing which can increase the power expenditure of the battery-operated UAVs.

Motivated by the above observations, this paper studies the effect of co-channel interference generated by multiple UAVs on the coverage area performance within a multi-UAV network, where the coverage area performance is defined as the ratio of the sum of effective coverage area of USCs to the target area as a function of the separation distance between UAVs. The multi-UAV network consists of a primary UAV surrounded by secondary UAVs operating in a coordinated framework in two scenarios. First, this work assumes the symmetric deployment of UAVs that have the same optimal altitude and transmit power. Second, in the asymmetric deployment of UAVs, a primary UAV is placed at an optimal altitude and secondary UAVs are located above and below the optimal altitude with different transmit power. In both cases, the worst-case scenario of the co-channel interference generated by UAVs is considered. The optimal separation distance for a given target area with predefined signal-to-interference-plus-noise ratio (SINR) is studied. Numerical results show that the coverage area performance depends on the SINR threshold, the separation distance between UAVs, and the number of UAVs and their formations.

## B. CONTRIBUTIONS AND ORGANIZATION

The main contributions of this paper are summarized as follows:

- 1) Different from [9] and [10], which does not include the effects of co-channel interference between multiple UAVs in the placement optimization problem, this paper proposes a coordinated multi-UAV framework to study the coverage area performance in presence of co-channel interference. Specifically, multiple UAVs are deployed at the predefined coordinates in a two-dimensional (2D) Cartesian plane by exploiting hexagonal layout. These coordinates are specified for a minimum UAV separation distance to avoid collision in a given target area and utilize SNR measures to find the optimal altitude of UAVs.
- 2) After the initial deployment of UAVs at the specific coordinates and the optimal altitude, this paper characterizes the impact of the UAV separation distance on the coverage area optimization in the presence of co-channel interference with the help of SINR metrics to meet the threshold requirement for the worst-case scenario. Compared with [16], this work studies the coverage area performance for multiple UAVs that can be deployed in one-dimensional (1D) or 2D formations in a single snapshot, while [16] only considered two UAVs deployed in 1D formations. Also, compared with the circle packing approach in [20] and the circle placement approach in [22], this work considers the realistic overlapping scenario of USCs which results in the reduction of the effective coverage area due to the interference and consequently the shape of USCs varies according to the separation distance between UAVs. The results then provides the useful insights for enabling an harmonious integration of multiple USCs in UAV communications.
- 3) Using the proposed UAV deployment framework, this paper analyzes the system-level performance in terms of the coverage probability of the ground user located at the boundary of the USC with the maximum coverage distance. The results are then used to determine the minimum number of UAVs needed to achieve a target coverage probability at different UAV separation distances.

The rest of this paper is organized as follows. The system model is introduced in Section II, including the use of the practical channel model. Section III presents the framework for the deployment of multi-UAV network and assesses the coverage area performance and the coverage probability in presence of interference. Section IV presents numerical results. Section V summarizes the main conclusions of this paper.

## II. SYSTEM MODEL

Coordinated multi-UAV network can be used to alleviate the co-channel interference in UAV communications. As a general multiple UAV model for  $M$  aerial base stations, this

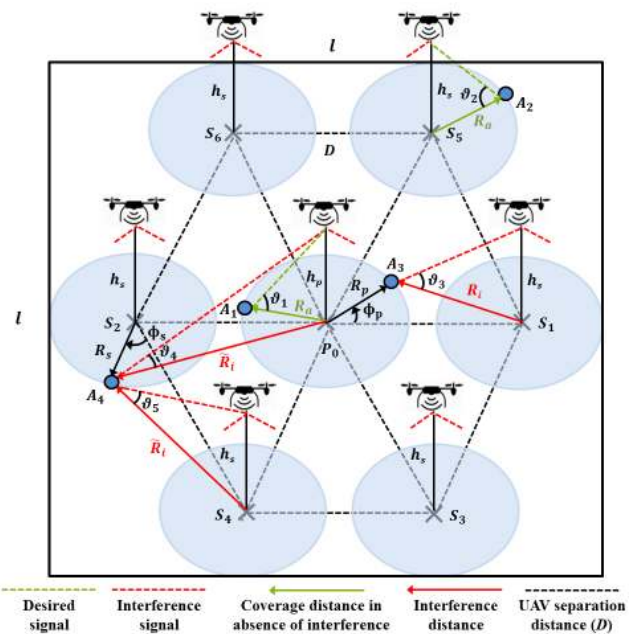


FIGURE 1. Diagram of the multiple interfering UAVs scenario.

work assumes that the primary UAV is static and fixed on top of the center of a specified target area to serve as a reference node to adjust the separation distance, while secondary UAVs are placed at the predefined deployment coordinates. The secondary UAVs in this work are static after optimization so that the coverage is also static on the ground. Fig. 1 depicts a downlink UAV transmission system that consists of the primary UAV and secondary UAVs positioned at an altitude of  $h_p$  and  $h_s$  meters, respectively. Without loss of generality, a two-dimensional (2D) Cartesian system is considered in which seven UAVs are used in the Euclidean plane of the square target area with a side length of  $l$  meters and assume hexagonal layout for UAV deployment. It should be noted that the use of seven UAVs in Fig. 1 is only for illustration purpose. The model is applicable to any numbers of UAVs but in practice, large numbers are highly unlikely due to the exponentially increasing complexity for UAV control, such as collision avoidance and ground coordination. In this case,  $P_0$  is the projection center of the primary UAV and  $S_1, \dots, S_{M-1}$  are the coordinates of secondary UAVs located at the vertices, where  $M = 7$  in Fig. 1. As a result, spatial isolation between interfering UAVs is possible with the same separation distance  $D$ . Moreover, coordinated multi-UAV networks can be deployed based on the layout of regular convex polygons to meet the coverage requirement inside the specific target area with the required number of UAVs. The advantage of such coordinated scheme is that it can react to failure of any UAVs quickly by reformation of the deployment strategy to the nearest regular polygon layout. The considered multi-UAV network offers resiliency of wireless network in case of malfunctioning base stations and providing coverage in post-disaster areas.

In the absence of interference,  $R_a$  is the maximum coverage distance at the boundary points  $A_1$  and  $A_2$  in the primary and secondary USC, respectively. In the presence of interference,  $R_p$  and  $R_s$  are coverage distances that attain a minimum performance, respectively, for boundary points  $A_3$  and  $A_4$  in the primary and secondary USC.  $R_{i \in \{1, \dots, M-1\}}$  are distances to represent the worst-case scenario of the co-channel interference generated at the boundary of the primary USC from the projection of  $M - 1$  secondary UAVs. Also,  $\tilde{R}_{i \in \{1, \dots, M-1\}}$  denote the interference distances from the boundary point of the serving secondary USC to the coordinates of all remaining UAVs in the network. The coverage performances of both the primary and secondary UAVs are dependent on  $R_p$  and  $R_s$  as a function of  $D$  for a specific range of coverage angles, respectively,  $\Phi_p$  and  $\Phi_s$ .

**A. CHANNEL MODEL**

In this paper, the realistic channel model is used in which air-to-ground (AG) path-loss is modeled with both line-of-sight (LOS) and non line-of-sight (NLOS) components. To this end, one of the most suitable channel model was proposed in [3], which is predominantly utilized in the literature to facilitate the optimization of UAV placement in [4], [5], [7], [8], [10], [16], [20], [22], and [32]. This model considers the effect of the environment with parameters  $\alpha$  and  $\beta$  to characterize the AG propagation with the probability of LOS as

$$P_x = \frac{1}{1 + \alpha \times e^{(\alpha\beta - \beta\vartheta_x)}}, \tag{1}$$

where  $x \in \{1, 2, 3, 4, 5\}$  represents elevation angles  $\vartheta_1, \vartheta_2, \vartheta_3, \vartheta_4$ , and  $\vartheta_5$  at boundary points in five scenarios shown in Fig. 1. In the case of non-interfering link, the elevation angle for the primary UAV at point  $A_1$  is  $\vartheta_1 = \frac{180}{\pi} \arctan(\frac{h_p}{R_a})$  and the mean path loss is given as [32]

$$L_p(dB) = A \times P_1 + 10 \log_{10}(h_p^2 + R_a^2) + B. \tag{2}$$

The elevation angle for secondary UAV at point  $A_2$  is  $\vartheta_2 = \frac{180}{\pi} \arctan(\frac{h_s}{R_a})$  and the mean path loss is given as

$$L_s(dB) = A \times P_2 + 10 \log_{10}(h_s^2 + R_a^2) + B. \tag{3}$$

For the interference received in the primary USC at the boundary point  $A_3$  from secondary UAVs,  $\vartheta_3 = \frac{180}{\pi} \arctan(\frac{h_i}{R_i})$  for  $i = \{1, 2, \dots, M - 1\}$  and the mean path loss is given as

$$L_i(dB) = A \times P_3 + 10 \log_{10}(h_s^2 + R_i^2) + B. \tag{4}$$

For the interference incurred in the serving secondary USC at point  $A_4$  by the primary UAV, the interference distance between projection coordinate  $P_0$  and boundary point  $A_4$  is  $\tilde{R}_{i=1}$ . Therefore,  $\vartheta_4 = \frac{180}{\pi} \arctan(\frac{h_p}{\tilde{R}_{i=1}})$  and the mean path loss is given as

$$\tilde{L}_{i=1}(dB) = A \times P_4 + 10 \log_{10}(h_p^2 + \tilde{R}_{i=1}^2) + B. \tag{5}$$

For the interference received in the same secondary USC at point  $A_4$  from the remaining secondary UAVs,

$\vartheta_5 = \frac{180}{\pi} \arctan(\frac{h_s}{\tilde{R}_i})$  for  $i = \{2, \dots, M - 1\}$  and the mean path loss is given as

$$\tilde{L}_i(dB) = A \times P_5 + 10 \log_{10}(h_s^2 + \tilde{R}_i^2) + B. \tag{6}$$

where  $A = \xi_{LOS} - \xi_{NLOS}$ ,  $B = 20 \log(\frac{4\pi f}{c}) + \xi_{NLOS}$ ,  $\xi_{LOS}$  and  $\xi_{NLOS}$  denote the excessive path loss factors which rely on the propagation environment as well as on the LOS and NLOS conditions, respectively. Also,  $f$  is the carrier frequency and  $c$  is the speed of light.

The above channel model is considered due to its commonality in the formulation of the optimization problem for UAV placement. In addition, the system parameters and channel characteristics are the same for all UAVs. Next,  $L_s$  and  $L_p$  will be used to present SNR measures. Also,  $L_i, \tilde{L}_{i=1}$ , and  $\tilde{L}_i$  will be used for SINR metrics.

**III. COVERAGE AREA PERFORMANCE OF COORDINATED MULTI-UAV NETWORK**

Interference control is one of the major challenges in radio resource management of UAV communications. Intuitively, it is evident from the considered system model that, in the absence of coordination between UAVs, a large value of  $D$  would deteriorate the coverage performance by moving the coverage areas of multiple UAVs outside the boundary of the target area but leave a big gap between them for protection. Conversely, a small value of  $D$  leads to the overlap of USC areas to provide more coverage but cause strong co-channel interference when all participating UAVs use the same frequency resources at the same time. Therefore, the optimal separation distance between UAVs exists and provides trade-off between interference avoidance and maximum coverage. This section defines the deployment strategy for the considered multi-UAV system and then employs it to present the coverage area performance and the coverage probability as a function of the UAV separation distance.

**A. UAV ALTITUDE**

Fig. 2 illustrate the cases of symmetric and asymmetric deployments based on UAV altitude. In the symmetric case, the altitudes and transmit powers of all UAVs are identical. However, for asymmetric case, the primary UAV is placed at an optimal altitude and secondary UAVs can be located above or below this altitude. Therefore, the first goal of this work is to place the primary UAV at the optimal altitude  $h_p$  to achieve the maximum ground coverage in a specific target area for a given  $R_a$ . In this regard, the boundary point  $A_1$  on the ground is covered when its SNR is above a certain threshold  $\Psi_{th}$  for a minimum transmit power,  $P_{tp}$ , i.e.

$$SNR(R_a, h_p) = \frac{P_{r_p}}{N_0} \geq \Psi_{th}, \tag{7}$$

where  $P_{r_p} = P_{tp} \times 10^{\frac{-L_p}{10}}$  is the received power in the absence of interference,  $L_p$  is given in (2), and  $N_0$  is the noise power. The SNR for the secondary UAV is given as

$$SNR(R_a, h_s) = \frac{P_{r_s}}{N_0} \geq \Psi_{th}, \tag{8}$$

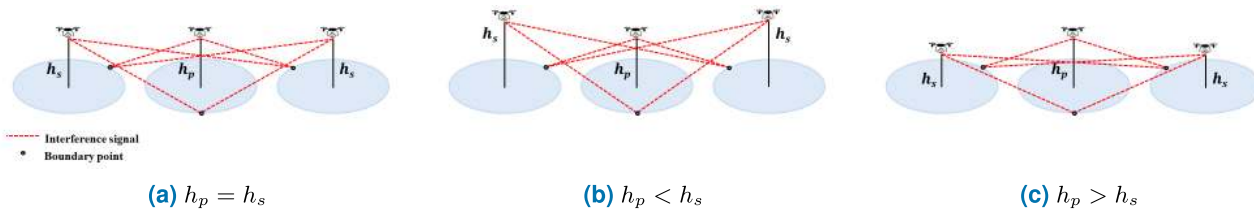


FIGURE 2. Illustration of symmetric and asymmetric UAV deployment scenarios.

where  $P_{r_s} = P_{t_s} \times 10^{-\frac{L_s}{10}}$  is the received power in the absence of interference,  $P_{t_s}$  is the corresponding transmit power of secondary UAVs at altitude  $h_s$ , and  $L_s$  is given in (3).

**B. PROJECTION COORDINATES**

This paper focuses on the use of quasi-stationary UAVs, where their positions remain unchanged for a specific duration of time. For such setup, it is important to determine the placement coordinates of UAVs to avoid collision between them and to provide spatial isolation between UAVs to control the interference. Therefore, the deployment strategy assumes that the primary UAV is fixed at  $P_0 = \{0, 0\}$ . When  $M = 7$ , the coordinates of secondary UAVs in the hexagonal layout are given as

$$S_{1, \dots, M-1} = \begin{cases} S_1(D_{min} + D, 0) \\ S_2(- (D_{min} + D), 0) \\ S_3(\frac{1}{2}(D_{min} + D), -\frac{\sqrt{3}}{2}(D_{min} + D)) \\ S_4(-\frac{1}{2}(D_{min} + D), -\frac{\sqrt{3}}{2}(D_{min} + D)) \\ S_5(\frac{1}{2}(D_{min} + D), \frac{\sqrt{3}}{2}(D_{min} + D)) \\ S_6(-\frac{1}{2}(D_{min} + D), \frac{\sqrt{3}}{2}(D_{min} + D)), \end{cases} \quad (9)$$

where  $D_{min} = \frac{L_s}{4} - R_a$  is the minimum separation distance to avoid collision between UAVs and to ensure minimum coverage performance for all participating UAVs in the presence of interference. In this case,  $D$  is the only variable which controls the coverage area performance within a target area.

**C. SIGNAL-TO-INTERFERENCE-PLUS-NOISE RATIO (SINR)**

SINR is a commonly used metric for wireless communication systems to characterize the impact of interference generated by adjacent base stations. This affects the received signal strength at a ground user and consequently defines the coverage area of the cell. This paper assumes that the participating UAVs in the considered system interfere with each other during the downlink transmission. In this case, a boundary user at point  $A_3$  is served by the primary UAV in the presence of interfering secondary UAVs when its SINR satisfies the threshold requirement  $\Psi_{th}$ . As a result, SINR can be defined as

$$SINR(R_p(D), \Phi_p) = \frac{P_{r_p}}{I + N_0} \geq \Psi_{th}, \quad (10)$$

where  $R_p$  is related to the interference distance  $R_i$  as

$$R_i = \sqrt{R_p^2 + D^2 + 2R_pD \cos(\pi - \Phi_p)}, \quad (11)$$

and  $I = P_{t_s} \sum_{i=1}^{M-1} 10^{-\frac{L_i}{10}}$  is the co-channel interference generated by secondary UAVs, and  $L_i$  is given in (4).

For the boundary point  $A_4$  in the secondary USC, the SINR is given as

$$SINR(R_s(D), \Phi_s) = \frac{P_{r_s}}{\tilde{I} + N_0} \geq \Psi_{th}, \quad (12)$$

where  $R_s$  is dependent on the interference distance  $\tilde{R}_i$  as

$$\tilde{R}_i = \sqrt{R_s^2 + D^2 + 2R_sD \cos(\pi - \Phi_s)}, \quad (13)$$

and  $\tilde{I} = P_{t_p} \times 10^{-\frac{\tilde{L}_{i=1}}{10}} + P_{t_s} \sum_{i=2}^{M-1} 10^{-\frac{\tilde{L}_i}{10}}$ ,  $\tilde{L}_{i=1}$  is given in (5), and  $\tilde{L}_i$  is given in (6).

**D. COVERAGE AREA PERFORMANCE AS A FUNCTION OF OPTIMAL SEPARATION DISTANCE**

The coverage area ratio determines the overall coverage area performance of the considered multi-UAV system. Particularly, it is defined as the ratio of the total effective area covered by both the primary and secondary USCs to the target area as

$$A_c(D) = \frac{2}{l^2} \left[ \int_0^{R_p(D)} \int_{\Phi_p=0}^{\Phi_p=\pi} R dR d\Phi + (M - 1) \int_0^{R_s(D)} \int_{\Phi_s=0}^{\Phi_s=\Phi_{max}} R dR d\Phi \right], \quad \Phi_{max} \leq \pi, \quad (14)$$

where  $l^2$  is the area of the square target area considered in the system model. Note that this work considers SINR measure which is dependent on the position of the ground user. Therefore, analytical expression for the coverage area ratio is too complicated to be derived. Following (14), the minimum coverage area ratio can be obtained at  $D = D_{min}$ . Also,  $\Phi_{max}$  limits the coverage of secondary UAVs that might project outside the target area and is given as

$$\Phi_{max} = \pi - \arccos\left\{\frac{D_{min} + D}{R_s}\right\}. \quad (15)$$

Finally, the optimal separation distance can be computed by searching (14) numerically as

$$D_{opt} = \arg \max_D A_c(D). \quad (16)$$

Analytical expressions for  $D_{opt}$  is difficult to obtain, if not impossible. Therefore, this work will use simulation to study the effect of  $D$  on  $A_c(D)$  and to determine  $D_{opt}$  for maximum coverage area ratio.

**E. COVERAGE PROBABILITY OF THE BOUNDARY USER**

The coverage probability is defined as

$$\mathbb{P}_c = \mathcal{P}[SINR \geq \Psi_{th}], \tag{17}$$

which can be written as  $\mathbb{P}_c = \mathcal{P}[SINR(D) \geq \Psi_{th}]$  as the SINR depends on the separation distance between UAVs and the threshold  $\Psi_{th}$  determined by the requirement of the ground user. This performance metric quantifies the reliability of the AG channel in presence of co-channel interference by satisfying the threshold requirement. In addition, this metric is useful to evaluate the performance of the AG channel for command and control (CnC) in multi-UAV network [33]. A reliable CnC is crucial for safe UAV deployment and better traffic management in UAV communications.

For the proposed coordinated multi-UAV network, the shape of the coverage regions of the primary and secondary UAVs may not be completely circular in the presence of the co-channel interference. As a result, the coverage distances  $R_p$  and  $R_s$  varies non-uniformly for the primary and secondary USCs, respectively, as the value of  $D$  changes. In this case, the severe interference can be observed at the boundary points of USCs. The coverage probability for a boundary user located at the maximum distance  $R_p$  from the projection of the primary UAV by considering the aggregate interference from all secondary UAVs is given as

$$\mathbb{P}_c = \mathcal{P}\left[\frac{P_{rp}}{I + N_0} \geq \Psi_{th}\right] = \mathcal{P}\left[P_{rp}(dB) \geq P_{min}\right]. \tag{18}$$

where  $\mathcal{P}[\cdot]$  denotes probability,  $P_{rp}$  is the received power in the absence of interference,  $P_{min} = 10 \log_{10}(\Psi_{th}I + \Psi_{th}N_0)$  is the minimum received power (in dB) for successful detection in presence of interference, and  $I$  can be extracted from (10). Similarly, the coverage probability can be determined for a ground user located at the maximum coverage distance  $R_s$  from the projection of the serving secondary UAV by considering aggregate interference from remaining UAVs by using (12).

**IV. NUMERICAL RESULTS AND DISCUSSION**

In this section, numerical results are presented. Simulation parameters for suburban and urban environments are listed in Table 1.

Fig. 3 shows the optimal altitude for the primary UAV using (7) to have the minimum transmit power in order to attain the coverage at the maximum radial distance of 350 meters and satisfy the threshold requirement of  $\Psi_{th} = 10$  dB. Actually, the optimal altitude is the minimum possible altitude which offers the lowest path-loss between the UAV and the ground user with the minimum transmit power. This leads to the best communication performance in the absence of interference. Fig. 3 also shows that the optimal altitude

**TABLE 1. Simulation parameters.**

Parameter	Value
$l$	2000 meters
$f$	2 GHz
$N_0$	-120 dBm
$\Psi_{th}$	10 dB
suburban ( $\xi_{LOS}, \xi_{NLOS}, \alpha, \beta$ )	0.1 dB, 21 dB, 4.88, 0.43
urban ( $\xi_{LOS}, \xi_{NLOS}, \alpha, \beta$ )	1 dB, 20 dB, 9.6, 0.28

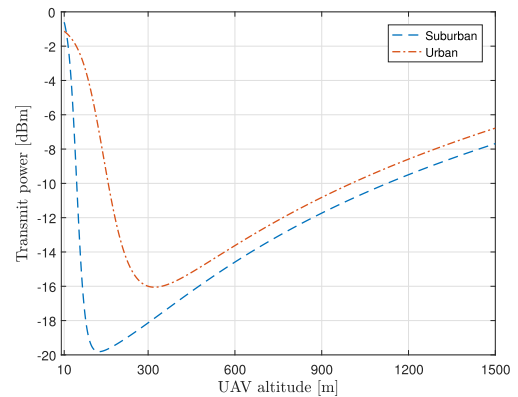


**FIGURE 3. UAV altitude versus transmit power for urban [16] and suburban environment with  $R_d = 350$  meters.**

and minimum transmit power depends on the propagation environment. For instance, the optimal altitude is 131 meters and 314 meters in suburban and urban scenarios, respectively. This result is important for the power minimization in planning multi-UAV networks.

Fig. 4 and Fig. 5 show the ground coverage pattern in a specific target area with different numbers of UAVs for the minimum and the maximum coverage, respectively, in suburban environment with the threshold of  $\Psi_{th} = 10$  dB and the optimal altitude of 131 meters for all UAVs. The projection coordinates of UAVs are marked by black 'x'. Particularly, Fig. 4(a) and Fig. 5(a) present the coverage of three UAVs placed along a single axis in one-dimensional (1D) formation with the separation distance of 247 meters and 747 meters, respectively. Fig. 4(b) and Fig. 5(b) depicts the coverage region of five UAVs deployed in 2D formation with the separation distance of 247 meters and 847 meters, respectively. Fig. 4(c) and Fig. 5(c) shows the coverage area of seven UAVs deployed in 2D formation with the separation distance of 247 meters and 847 meters, respectively. Expressions (10) and (12) are used to achieve the SINR requirements at the ground points for the coverage of different UAVs deployed at coordinates specified by (9). These results, use  $10^3$  sample points for individual UAVs to test ground coverage requirement and the green patches represent the coverage area of USCs that achieve the threshold requirement in the presence of interference. In this case, the separation distance of 747 meters in 1D formation and 847 meters in 2D formation compensates the strong co-channel interference because the maximum coverage area of the primary UAV

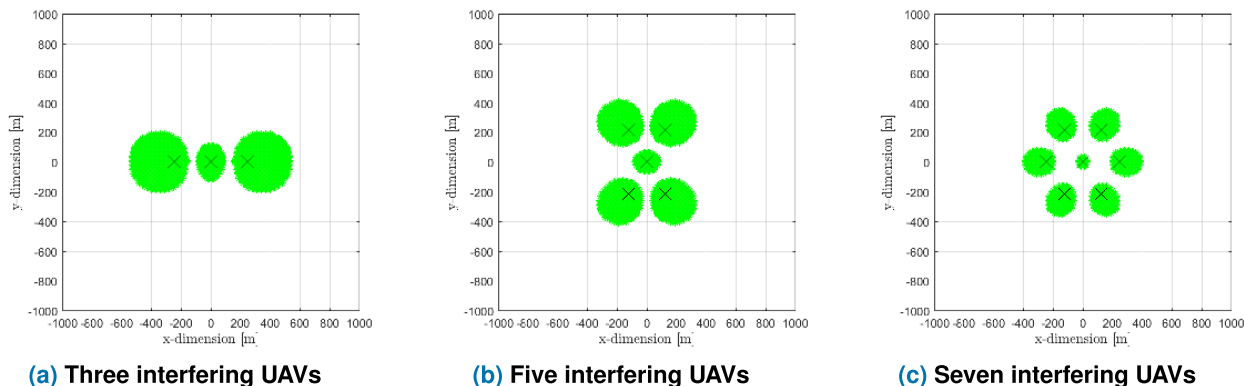


FIGURE 4. Coverage map for coordinated multi-UAV deployment for different numbers of UAVs in suburban environments to attain minimum coverage.

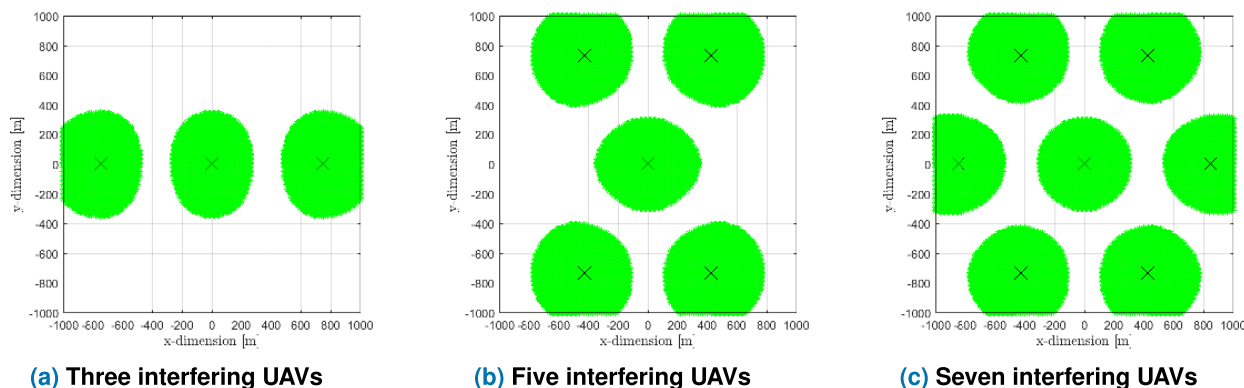


FIGURE 5. Coverage map for coordinated multi-UAV deployment for different numbers of UAVs in suburban environments to attain maximum coverage.

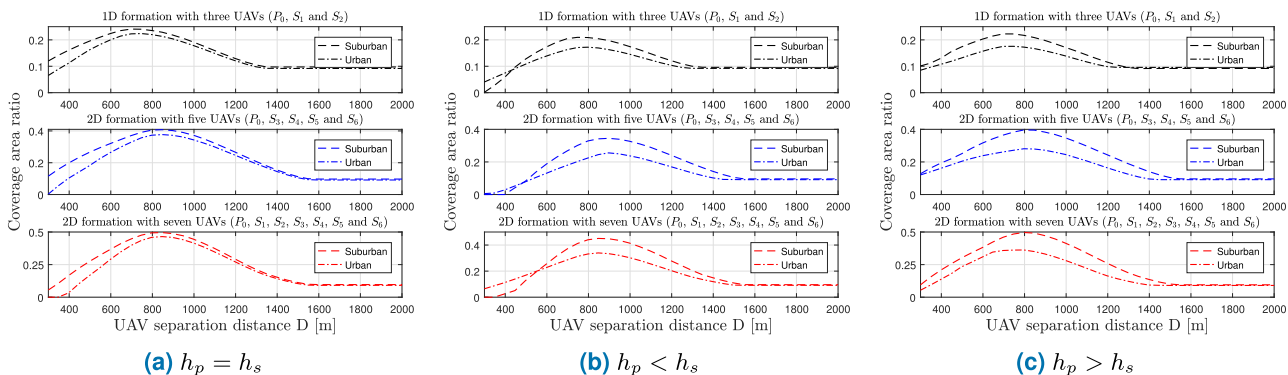


FIGURE 6. Coverage area ratio versus separation distance for different numbers of UAVs in suburban and urban environments.

is optimally confined within the target area, while a small portion of the coverage region of secondary UAVs falls outside the target area. Furthermore, as the gap between USC's increases beyond these separation distance, the coverage area of secondary UAVs further moves outside the target area which results in undesirable coverage leakage. On the other hand, the separation distance of 247 meters in both 1D and 2D formations can cause detrimental interference effect on the

coverage performance as the effective coverage area shrinks because of overlapping.

Fig. 6 shows the coverage performance as the ratio of the effective coverage area of USC's to the target area. In the simulation, 'fsolve' in MATLAB was used to find coverage distances  $R_p$  in (11) and  $R_s$  in (13) for the considered multi-UAV network and then apply them in (14)-(16) to observe the effect of the UAV separation distance on the coverage area

performance in suburban and urban environments. Clearly, to mitigate the interference and to improve the coverage performance with higher number of UAVs, the coverage regions of UAVs must be isolated with proper adjustment in the separation distance. One notices that the coverage ratio changes with the number of UAVs and the environmental conditions.

In Fig. 6(a), when using the optimal altitude i.e.  $h_p = h_s$ , better coverage performance is observed with three UAVs for  $D < 350$  meters in comparison with five and seven UAVs due to lessen co-channel interference. In contrast, for the case of  $h_p < h_s$  in Fig. 6(b), the coverage performance degrades as the altitude of secondary UAVs increased from the optimal value because of higher path-loss. For the case of  $h_p > h_s$  in Fig. 6(c), best coverage area ratio is observed for  $D < 500$  meters. However, as the separation distance increased from 500 meters the coverage performance becomes sub-optimal in urban environment. In these results, the minimum coverage area ratio is consistent with  $D = 1250$  meters and  $D = 1500$  meters for 1D and 2D formations, respectively, when the maximum coverage of primary USC is attained and secondary UAVs moved out of the target area. Furthermore, it is observed that to achieve the maximum coverage area ratio, the optimal separation distance is dependent on the deployment formation of UAVs rather on the number of UAVs or environment. For instance, with three UAVs deployed in the 1D formation, the optimal separation distance is 747 meters. Whereas, for five and seven UAVs deployed in 2D formation, the optimal separation distance is 847 meters.

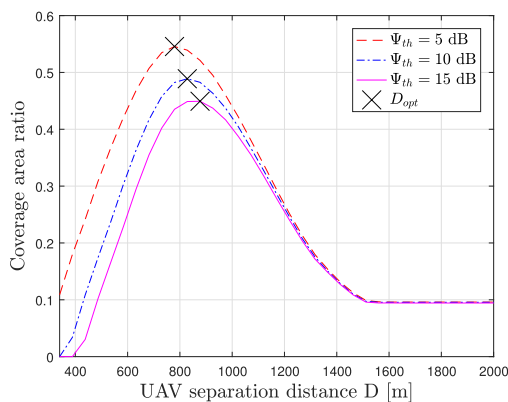


FIGURE 7. Coverage area ratio versus separation distance for seven UAVs deployed in urban environment with different SINR threshold.

Fig.7 illustrate the impact of the SINR threshold on the coverage ratio and the optimal UAV separation distance in the urban environment for seven interfering UAVs. According to Fig. 7, the optimal UAV separation distance increases with the SINR threshold. For example  $D_{opt} = 780$  meters for  $\Psi = 5$  dB,  $D_{opt} = 847$  meters for  $\Psi = 10$  dB, and  $D_{opt} = 897$  meters for  $\Psi = 15$  dB. On the other hand, the maximum coverage area ratio decreases as the SINR threshold increases. For example, the maximum coverage area ratio is 0.54 for  $\Psi = 5$  dB, 0.49 for  $\Psi = 10$  dB, and 0.45 for  $\Psi = 15$  dB.

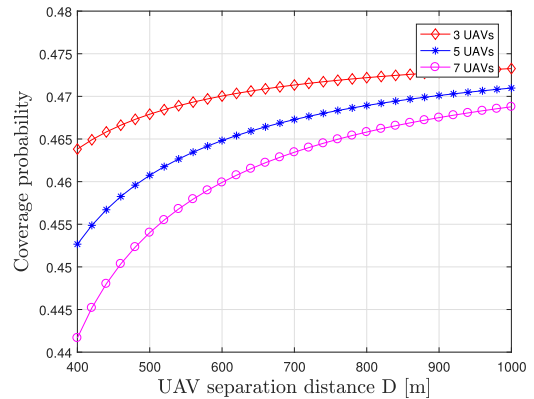


FIGURE 8. Boundary user coverage probability in the primary USC for the severe interference generated from secondary UAVs for different number of UAVs in urban environment.

Fig. 8 shows that the coverage probability of the boundary user in the primary UAV cell in (18) with the threshold of  $\Psi_{th} = 10$  dB. Fig 8. depicts that the user coverage probability improves as the separation distance increases. In this case, the better user performance is possible in the worst-case scenario of the co-channel interference with the minimum required number of UAVs.

These results show that the aerial base stations can work similarly as the ground base stations with defined coverage patterns following principles of coordinated multi-point systems for interference management [?]. This is important for the development of UAV base stations as a supplementary but flexible infrastructure to be compatible with existing fixed infrastructure.

## V. CONCLUSION

The optimal separation distance between UAVs to mitigate co-channel interference and maximize the overall coverage performance has been studied in suburban and urban environments. For this, the coordinated multi-UAV network was designed that allowed us to provide the useful insights on the integration of multiple USCs in UAV communications. Results in this paper showed that the coverage area performance is dependent on the number of UAVs, operational environment, deployment coordinates or network formation, and separation distance between UAVs. In fact, a proper adjustment of the UAV separation distance can balance the co-channel interference to avoid coverage leakage outside the target area. This work could be extended for UAVs with different mobility laws and a multiple-tier UAV deployment to study the consequences of cross-tier interference in UAV communications. In this case, coverage performance by multiple UAVs can be determined by multi-dimensional search for the optimal UAV altitudes and the separation distances.

## REFERENCES

[1] Y. Zeng, R. Zhang, and T. J. Lim, "Wireless communications with unmanned aerial vehicles: Opportunities and challenges," *IEEE Commun. Mag.*, vol. 54, no. 5, pp. 36–42, May 2016.

- [2] A. A. Khuwaja, Y. Chen, N. Zhao, M.-S. Alouini, and P. Dobbins, "A survey of channel modeling for UAV communications," *IEEE Commun. Surveys Tuts.*, vol. 20, no. 4, pp. 2804–2821, 4th Quart., 2018.
- [3] A. Al-Hourani, S. Kandeepan, and S. Lardner, "Optimal LAP altitude for maximum coverage," *IEEE Wireless Commun. Lett.*, vol. 3, no. 6, pp. 569–572, Dec. 2014.
- [4] A. Al-Hourani, S. Chandrasekharan, G. Kaandorp, W. Glenn, A. Jamalipour, and S. Kandeepan, "Coverage and rate analysis of aerial base stations," *IEEE Trans. Aerosp. Electron. Syst.*, vol. 52, no. 6, pp. 3077–3081, Dec. 2016.
- [5] M. Alzenad, A. El-Keyi, F. Lagum, and H. Yanikomeroglu, "3-D Placement of an unmanned aerial vehicle base station (UAV-BS) for energy-efficient maximal coverage," *IEEE Wireless Commun. Lett.*, vol. 6, no. 4, pp. 434–437, Aug. 2017.
- [6] M. M. Azari, F. Rosas, K.-C. Chen, and S. Pollin, "Optimal UAV positioning for terrestrial-aerial communication in presence of fading," in *Proc. IEEE GLOBECOM*, Dec. 2016, pp. 1–7.
- [7] Y. Chen, W. Feng, and G. Zheng, "Optimum placement of UAV as relays," *IEEE Commun. Lett.*, vol. 22, no. 2, pp. 248–251, Feb. 2018.
- [8] M. Alzenad, A. El-Keyi, and H. Yanikomeroglu, "3-D placement of an unmanned aerial vehicle base station for maximum coverage of users with different QoS requirements," *IEEE Wireless Commun. Lett.*, vol. 7, no. 1, pp. 38–41, Feb. 2018.
- [9] J. Lyu, Y. Zeng, R. Zhang, and T. J. Lim, "Placement optimization of UAV-mounted mobile base stations," *IEEE Commun. Lett.*, vol. 21, no. 3, pp. 604–607, Mar. 2017.
- [10] R. I. Bor-Yaliniz, A. El-Keyi, and H. Yanikomeroglu, "Efficient 3-D placement of an aerial base station in next generation cellular networks," in *Proc. IEEE ICC*, May 2016, pp. 1–5.
- [11] M. Mozaffari, W. Saad, M. Bennis, and M. Debbah, "Mobile Internet of Things: Can UAVs provide an energy-efficient mobile architecture?" in *Proc. IEEE GLOBECOM*, Dec. 2016, pp. 1–6.
- [12] S. Kumar, S. Suman, and S. De, "Backhaul and delay-aware placement of UAV-enabled base station," in *Proc. IEEE INFOCOM Workshops*, Apr. 2018, pp. 634–639.
- [13] M. Gruber, "Role of altitude when exploring optimal placement of UAV access points," in *Proc. IEEE WCNC*, Apr. 2016, pp. 1–5.
- [14] W. Feng, Y. Wang, D. Lin, N. Ge, J. Lu, and S. Li, "When mmWave communications meet network densification: A scalable interference coordination perspective," *IEEE J. Sel. Areas Commun.*, vol. 35, no. 7, pp. 1459–1471, Jul. 2017.
- [15] S. Rohde and C. Wietfeld, "Interference aware positioning of aerial relays for cell overload and outage compensation," in *Proc. IEEE VTC-Spring*, Sep. 2012, pp. 1–5.
- [16] M. Mozaffari, W. Saad, M. Bennis, and M. Debbah, "Drone small cells in the clouds: Design, deployment and performance analysis," in *Proc. IEEE GLOBECOM*, Dec. 2015, pp. 1–6.
- [17] B. Van Der Bergh, A. Chiumento, and S. Pollin, "LTE in the sky: Trading off propagation benefits with interference costs for aerial nodes," *IEEE Commun. Mag.*, vol. 54, no. 5, pp. 44–50, May 2016.
- [18] I. Kovacs, R. Amorim, H. C. Nguyen, J. Wigard, and P. Mogensen, "Interference analysis for UAV connectivity over LTE using aerial radio measurements," in *Proc. IEEE VTC-Fall*, Sep. 2017, pp. 1–6.
- [19] D. G. Cileo, N. Sharma, and M. Magarini, "Coverage, capacity and interference analysis for an aerial base station in different environments," in *Proc. ISWCS*, Aug. 2017, pp. 281–286.
- [20] M. Mozaffari, W. Saad, M. Bennis, and M. Debbah, "Efficient deployment of multiple unmanned aerial vehicles for optimal wireless coverage," *IEEE Commun. Lett.*, vol. 20, no. 8, pp. 1647–1650, Aug. 2016.
- [21] N. Zhao, F. Cheng, F. R. Yu, J. Tang, Y. Chen, G. Gui, and H. Sari, "Caching UAV assisted secure transmission in hyper-dense networks based on interference alignment," *IEEE Trans. Commun.*, vol. 66, no. 5, pp. 2281–2294, May 2018.
- [22] J. Sun and C. Masouros, "Deployment strategies of multiple aerial BSs for user coverage and power efficiency maximization," *IEEE Trans. Commun.*, vol. 67, no. 4, pp. 2981–2994, Apr. 2019.
- [23] Q. Wu, Y. Zeng, and R. Zhang, "Joint trajectory and communication design for multi-UAV enabled wireless networks," *IEEE Trans. Wireless Commun.*, vol. 17, no. 3, pp. 2109–2121, Mar. 2018.
- [24] F. Jiang and A. L. Swindlehurst, "Optimization of UAV heading for the ground-to-air uplink," *IEEE J. Sel. Areas Commun.*, vol. 30, no. 5, pp. 993–1005, Jun. 2012.
- [25] M. M. Azari, Y. Murillo, O. Amin, F. Rosas, M.-S. Alouini, and S. Pollin, "Coverage maximization for a poisson field of drone cells," in *Proc. PIMRC*, Oct. 2017, pp. 1–6.
- [26] L. Liu, S. Zhang, and R. Zhang, "Cooperative interference cancellation for multi-beam UAV uplink communication: A DoF analysis," in *Proc. IEEE GLOBECOM*, Dec. 2018, pp. 1–6.
- [27] N. Zhao, X. Liu, F. R. Yu, M. Li, and V. C. M. Leung, "Communications, caching, and computing oriented small cell networks with interference alignment," *IEEE Commun. Mag.*, vol. 54, no. 9, pp. 29–35, Sep. 2016.
- [28] F. Cheng, Y. Yu, Z. Zhao, N. Zhao, Y. Chen, and H. Lin, "Power allocation for cache-aided small-cell networks with limited backhaul," *IEEE Access*, vol. 5, pp. 1272–1283, 2017.
- [29] L. Liu, S. Zhang, and R. Zhang, "CoMP in the sky: UAV placement and movement optimization for multi-user communications," *IEEE Trans. Commun.*, to be published.
- [30] U. Challita, W. Saad, and C. Bettstetter, "Interference management for cellular-connected UAVs: A deep reinforcement learning approach," *IEEE Trans. Wireless Commun.*, vol. 18, no. 4, pp. 2125–2140, Apr. 2019.
- [31] W. Mei and R. Zhang, "Uplink cooperative NOMA for cellular-connected UAV," *IEEE J. Sel. Areas Commun.*, vol. 13, no. 3, pp. 644–656, Jun. 2019.
- [32] W. Feng, J. Wang, Y. Chen, X. Wang, N. Ge, and J. Lu, "UAV-aided MIMO communications for 5G Internet of Things," *IEEE Internet Things J.*, vol. 6, no. 2, pp. 1731–1740, Apr. 2019.
- [33] M. M. Azari, F. Rosas, and S. Pollin, "Cellular connectivity for UAVs: Network modeling, performance analysis and design guidelines," *IEEE Trans. Wireless Commun.*, to be published.
- [34] S. Sun, Q. Gao, Y. Peng, Y. Wang, and L. Song, "Interference management through CoMP in 3GPP LTE-advanced networks," *IEEE Wireless Commun.*, vol. 20, no. 1, pp. 59–66, Feb. 2013.



**AZIZ A. KHUWAJA** received the B.E. degree in telecommunication engineering from the Mehran University of Engineering and Technology, Jamshoro, Pakistan, in 2010, and the M.Sc. degree in electronics communication and computer engineering from the University of Nottingham, U.K., in 2015. He is currently pursuing the Ph.D. degree in engineering with the School of Engineering, The University of Warwick, U.K. He is also as an Assistant Professor with the Department of Electrical Engineering, Sukkur IBA University, Sukkur, Pakistan. His research interests include wireless communications and radio resource management in UAV communications.



**GAN ZHENG** (S'05–M'09–SM'12) received the B.Eng. and M.Eng. degrees in electronic and information engineering from Tianjin University, Tianjin, China, in 2002 and 2004, respectively, and the Ph.D. degree in electrical and electronic engineering from The University of Hong Kong, in 2008. He is currently a Reader of signal processing for wireless communications with the Wolfson School of Mechanical, Electrical and Manufacturing Engineering, Loughborough University, U.K. His research interests include machine learning for communications, UAV communications, edge caching, full-duplex radio, and wireless power transfer. He was the first recipient of the 2013 IEEE Signal Processing Letters Best Paper Award. He received the 2015 GLOBECOM Best Paper Award and the 2018 IEEE Technical Committee on Green Communications & Computing Best Paper Award. He currently serves as an Associate Editor for the IEEE COMMUNICATIONS LETTERS.



**YUNFEI CHEN** (S'02–M'06–SM'10) received the B.E. and M.E. degrees in electronics engineering from Shanghai Jiao Tong University, Shanghai, China, in 1998 and 2001, respectively, and the Ph.D. degree from the University of Alberta, in 2006. He is currently an Associate Professor with The University of Warwick, U.K. His research interests include wireless communications, cognitive radios, wireless relaying, and energy harvesting.



**WEI FENG** (S'06–M'10–SM'19) received the B.S. and Ph.D. degrees (Hons.) from the Department of Electronic Engineering, Tsinghua University, Beijing, China, in 2005 and 2010, respectively. From 2010 to 2011, he was the Project Director of the National Science and Technology Major Project Management Office, Tsinghua University. From 2011 to 2014, he was a Postdoctoral Research Fellow with the Department of Electronic Engineering, Tsinghua University, where he has been an Assistant Professor, since 2014, and, then, an Associate Professor, since 2016. His research interests include maritime broadband communication networks, large-scale distributed antenna systems, and coordinated satellite-terrestrial networks. He received the Outstanding Ph.D. Graduate of Tsinghua University Award, in 2010, the IEEE WCSP Best Paper Award, in 2013, the First Prize of Science and Technology Award of China Institute of Communications, in 2015, the IEEE WCSP Best Paper Award, in 2015, and the Second Prize of National Technological Invention Award of China, in 2016. He currently serves as an Assistant to the Editor-in-Chief of *China Communications*.

• • •